

ELM Suppression and Pedestal Structure in I-Mode Plasmas on Alcator C-Mod

by

John Reel Walk, Jr.

S.B. Physics & Mathematics (2010)
Massachusetts Institute of Technology

Submitted to the Department of Nuclear Science and Engineering
in partial fulfillment of the requirements for the degree of

Doctor of Philosophy in Applied Plasma Physics

at the

MASSACHUSETTS INSTITUTE OF TECHNOLOGY

June 2014

© Massachusetts Institute of Technology 2014. All rights reserved.

Author
Department of Nuclear Science and Engineering
January 7, 2014

Certified by.....
Jerry W. Hughes
Research Scientist, Plasma Science and Fusion Center
Thesis Supervisor

Certified by.....
Dennis G. Whyte
Professor, Department of Nuclear Science and Engineering
Thesis Reader

Accepted by
Mujid S. Kazimi
TEPCO Professor of Nuclear Engineering
Chair, Department Committee on Graduate Students

ELM Suppression and Pedestal Structure in I-Mode Plasmas on Alcator C-Mod

by
John Reel Walk, Jr.

Submitted to the Department of Nuclear Science and Engineering
on January 7, 2014, in partial fulfillment of the
requirements for the degree of
Doctor of Philosophy in Applied Plasma Physics

Abstract

Abstract goes here.

Thesis Supervisor: Jerry W. Hughes
Research Scientist, Plasma Science and Fusion Center

Thesis Reader: Dennis G. Whyte
Professor, Department of Nuclear Science and Engineering

A dedication goes here maybe?

ACKNOWLEDGMENTS

Acknowledgements go here.

CONTENTS

1	INTRODUCTION	11
1.1	Plasmas for Fusion	12
1.1.1	Plasma Parameters	12
1.1.2	Fusion Fuels	13
1.2	Magnetic Confinement	16
1.2.1	Basic Principles	16
1.2.2	Toroidal Configurations	19
1.3	Alcator C-Mod	19
1.4	Confinement & Transport	21
1.4.1	Global Confinement	21
1.4.2	Transport Barriers	21
1.5	High-Performance Regimes	21
1.5.1	ELMy H-Mode	21
1.5.2	EDA H-Mode	21
1.5.3	I-Mode	21
1.6	Goals & Outline	21

LIST OF FIGURES

- Figure 1.1 Binding energy per nucleon versus atomic mass number, with notable isotopes marked. Reactions forming nuclei with higher binding energy per nucleon are exothermic – thus, fusion of elements lighter than ^{56}Fe or fission of elements heavier than ^{56}Fe releases energy. [9] 14
- Figure 1.2 Reaction rate normalized to fuel density, expressed as the rate coefficient $\langle\sigma v\rangle$, for fusion fuels as a function of temperature. Notably, deuterium-tritium fusion exhibits a higher peak reaction rate, as well as reaching that peak at a lower temperature, than other fuels. 15
- Figure 1.3 Electron and ion gyro orbits in an applied magnetic field. Note that, due to the charge dependence in the Lorentz Force (eq. (1.14)), electrons and ions orbit in opposite directions relative to the magnetic field. 17
- Figure 1.4 Cutaway view of the Alcator C-Mod tokamak, including cryostat and ancillary structures, illustrating the extensive support structures necessary for compact, high-field operation. 20

LIST OF TABLES

- Table 1 Summary of Alcator C-Mod typical operating parameters. 19

INTRODUCTION

The population of the earth is projected to increase substantially over the next half-century, potentially reaching as high as 10 billion globally by 2050 [1]. At the same time, any attempt to increase the quality of life of the existing population will necessarily involve increased energy consumption per capita, with a greater fraction of the earth approaching “first-world” consumption levels [2]. As such, worldwide energy consumption will likely continue to increase in the next few decades [3, 4]

This increase in energy demand occurs in parallel with increased pressure on traditional energy sources. Fossil fuels (oil, coal, and natural gas), while reliable sources of base-load power, nevertheless face issues. Oil faces increasing cost and technical difficulty in capturing dwindling available reserves, as well as the potential for serious ecological damage from accidents (e. g., the Deepwater Horizon offshore rig accident in 2010). Coal, while more readily available (an estimated 257 billion tons of recoverable reserves in the US, lasting roughly 240 years at current consumption [4, 5]), releases particulate matter into the atmosphere, with serious consequences both to the environment and to human health, as well as the greenhouse gases tied to deleterious climate change.

Renewable energy sources have a certain “green” appeal, but each is subject to strict limitations on their implementation. Solar and wind power suffer from a large degree of variability in their output, necessitating a combination of expensive energy storage methods or (often fossil-fuel based) backup production to handle shortfalls. Hydroelectric and geothermal power are suitable for base-load power production, but are strictly restricted in their implementation by geographic concerns – bluntly, there are relatively few locations where hydro or geothermal power generation is possible, and many of these have already been developed .

cite for this?

Conventional – that is, fission-based – nuclear power can also supply carbon-free base-load power, with fuel reserves lasting through the next century. While nuclear power does suffer from the potential for extremely serious accidents (Fukushima, Chernobyl) it is, in general, highly safe. However, public perception of nuclear power hinges on these safety concerns, limiting the expansion of nuclear power to meet increasing demand and the safe long-term handling of existing nuclear waste, as well as, ironically, preventing the replacement of an aging reactor fleet with newer, safer designs.

Fusion, the nuclear process driving stellar cores, is a potentially highly attractive option for satisfying the world’s growing energy needs in an efficient, environmentally-sound manner. A fusion reactor would supply base-load power using only a small amount of an effectively inexhaustible fuel (readily available for harvesting from seawater), with no greenhouse gas emissions or meaningfully radioactive waste, and the physical impossibility of a major “meltdown” accident. However, fusion remains in the experimental stage, with significant technical hurdles remaining before the development of a prototype fusion power plant. This thesis will attempt to contribute to the understanding of one of these hurdles, regarding the requirement for efficient plasma behavior in a reactor scenario **reword this!** Further reading on the development of fusion energy is available to the interested reader in several excellent references. [6, 7, 8] •

1.1 PLASMAS FOR FUSION

A *plasma* is a gas to which sufficient energy has been applied to strip some or all of the electrons off the nuclei of its constituent atoms. These ions and electrons freely interact with one another, behaving as coupled fluids. Plasmas of interest for fusion research are comprised of light elements (typically Hydrogen or Helium), and are at extremely high temperatures, in excess of 100 million Kelvin (10 – 20 keV). As these conditions are far in excess of the ionization energy for these elements, the plasma is dominated by collisions between its charged particles, rather than interactions with bound electron states.

1.1.1 Plasma Parameters

As the plasma is comprised of free charged particles, it responds strongly to electric and magnetic fields. In the presence of a DC electric field (externally applied, or generated by an imbalance of positive and negative charge in the plasma), the plasma will rearrange itself to screen out the field. This effect breaks down at short length scales, at which there is an insufficient number of charge carriers to rearrange and counter the field – the characteristic scale for this effect is the Debye Length, given by

$$\lambda_D = \sqrt{\frac{\epsilon_0 T}{ne^2}} \quad (1.1)$$

At size scales significantly larger than λ_D , this will enforce an approximately balanced electric charge in the plasma, termed “quasi-

neutrality". This is reflected in the number densities of electrons and multiple ion species j , each with charge Z_j , by the relation

$$n_e = \sum_j n_j Z_j \quad (1.2)$$

In a multiple-ion species plasma, we may also define an effective ion charge

$$Z_{\text{eff}} = \frac{1}{n_e} \sum_j n_j Z_j^2 \quad (1.3)$$

The electrostatic force driving this charge redistribution induces a "ringing" oscillation in the plasma, at the characteristic plasma frequency ω_p :

$$\omega_p = \sqrt{\frac{n_e e^2}{\epsilon_0 m_e}} \quad (1.4)$$

This natural oscillation in the plasma also has the effect of screening AC electric fields varying at frequencies $\omega < \omega_p$.

Coulomb collisions between charged particles in the plasma tend to drive magnetically-confined plasmas into thermal equilibrium, with the velocity distribution for a species given by the Maxwellian

$$f(v) = n \left(\frac{m}{2\pi T} \right)^{3/2} \exp \left(-\frac{mv^2}{2T} \right) \quad (1.5)$$

These collisions also cause the plasma to emit a continuous spectrum of Bremsstrahlung radiation. For a plasma in thermal equilibrium, integration over the full spectrum gives for the total radiated power

$$P_{\text{Brems}} = (5.35 \times 10^{-37}) n_e^2 Z_{\text{eff}}^2 \sqrt{T} \quad (1.6)$$

representing a consistent source of heat loss from the plasma.

1.1.2 Fusion Fuels

Fusion collectively refers to the class of nuclear reactions merging lighter nuclei into a single heavier element. While fusion reactions for elements lighter than iron are generally exothermic, as they form nuclei with greater binding energy per nucleon (see fig. 1.1), the most common and readily attainable involve isotopes of hydrogen or helium, the most promising candidates for which are shown below.

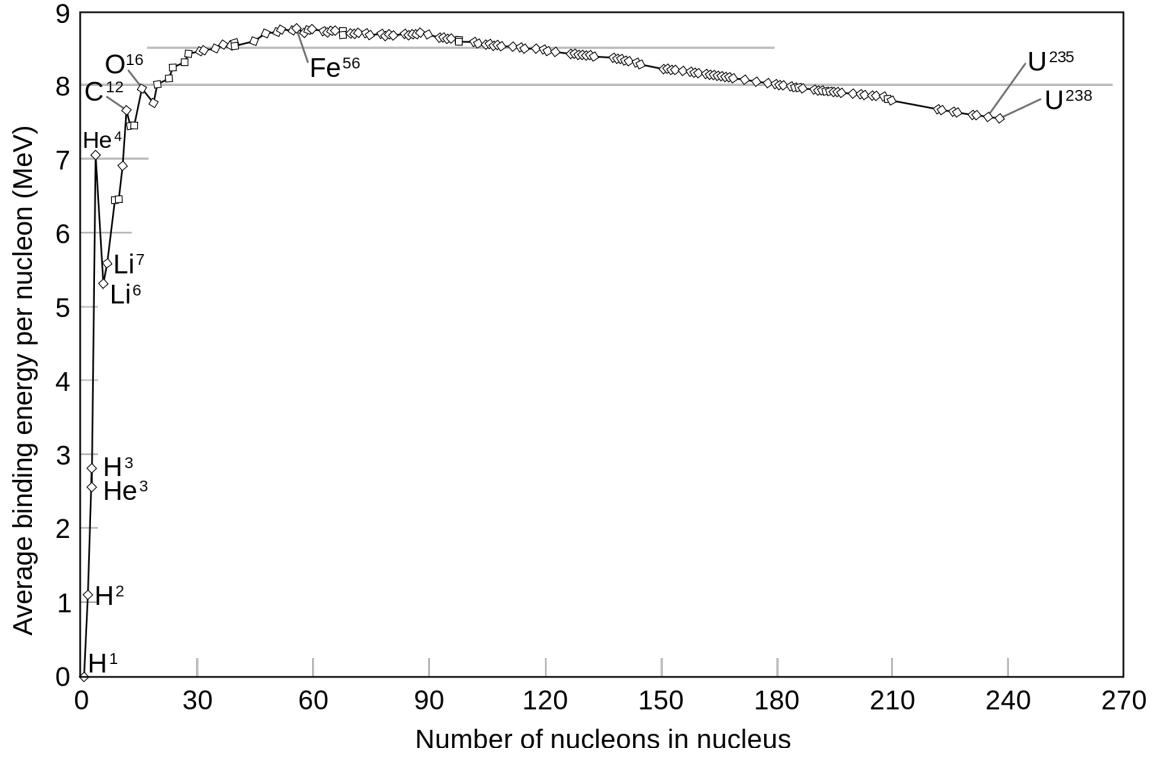
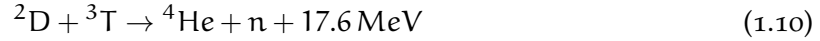
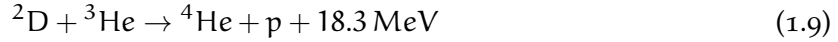
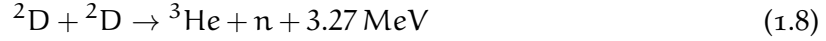


Figure 1.1: Binding energy per nucleon versus atomic mass number, with notable isotopes marked. Reactions forming nuclei with higher binding energy per nucleon are exothermic – thus, fusion of elements lighter than ^{56}Fe or fission of elements heavier than ^{56}Fe releases energy. [9]



Here D and T indicate nuclei of deuterium and tritium, two heavy isotopes of hydrogen (one proton plus one and two neutrons, respectively). The fusion reaction rate R_f is given by

$$R_f = n_1 n_2 \langle \sigma v \rangle_{1,2} \quad (1.11)$$

where n_1 and n_2 indicate the densities of the two fuel ions (e. g., for deuterium-tritium fuel $n_1 n_2 = n_{\text{D}} n_{\text{T}}$, while for pure-deuterium fuel $n_1 n_2 = \frac{1}{2} n_{\text{D}}^2$ to remove double-counting of fuel ions) and $\langle \sigma v \rangle_{1,2}$ is a rate parameter incorporating the energy-dependent reaction cross-section averaged over the Maxwellian fuel distribution (eq. (1.5)). In practice, the energy-dependent cross-section is empirically determined – measured rate parameters $\langle \sigma v \rangle$ for the fuels of interest are shown in fig. 1.2.

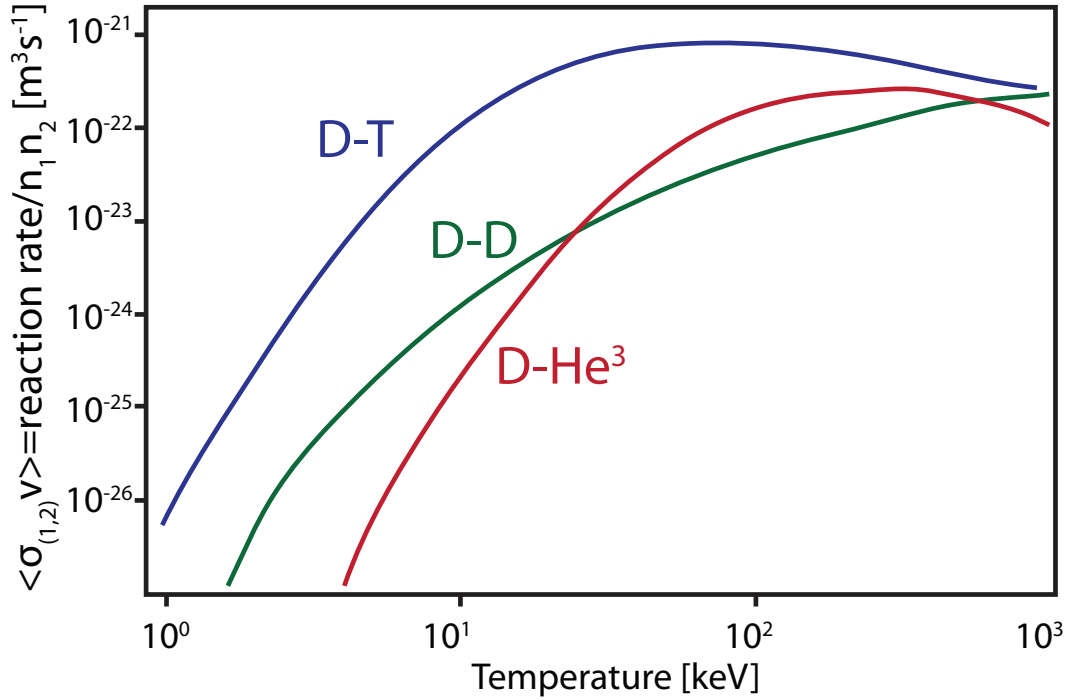


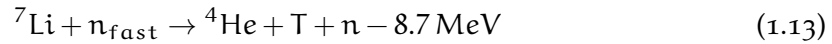
Figure 1.2: Reaction rate normalized to fuel density, expressed as the rate coefficient $\langle \sigma v \rangle$, for fusion fuels as a function of temperature. Notably, deuterium-tritium fusion exhibits a higher peak reaction rate, as well as reaching that peak at a lower temperature, than other fuels.

Pure deuterium fuel (reactions shown in eqs. (1.7) and (1.8)) is attractive from a research standpoint, due to the abundance and ease of use of deuterium. Deuterium is a stable nucleus, obviating the need for radiation safety in the fuel system, and is naturally occurring in relative abundance (approximately 1/6420 of hydrogen nuclei on earth are deuterium [cite](#)), allowing harvesting of deuterium fuel from seawater. However, pure-deuterium reactions suffer from low energy output per reaction and a significantly lower reaction rate at feasible plasma conditions compared to other fuel options (see fig. 1.2), setting high performance requirements for a putative DD-burning reactor.

The D – He³ reaction (eq. (1.9)) exhibits several desirable properties, namely an impressive energy yield per reaction, and the fact that the reaction produces only charged particles rather than the high-energy neutrons found in D – D and D – T reactions, which can cause significant damage to reactor materials. However, as with D – D fuel, the D – He³ reaction suffers from a lower reaction rate at attainable conditions, as well as the fact that Helium-3 does not occur in economically usable quantities on Earth. While off-planet sources of Helium-3 exist (for example, a useful quantity is present in the lunar regolith [cite](#)), this fuel remains the subject of speculation.

The deuterium-tritium reaction (eq. (1.10)) is considered the most promising for a first-generation fusion reactor, due to its high energy

output per reaction and favorable reaction cross-section – the rate parameter $\langle\sigma v\rangle_{DT}$ reaches its peak at a lower temperature, and reaches a greater absolute level than other fusion fuels. However, D – T operation is limited both by fuel sources, and reaction products. D – T fusion produces a 14 MeV neutron, carrying roughly 80% of the energy released by the fusion reaction, which can damage unshielded reactor materials. Moreover, while deuterium is stable and readily available, tritium is radioactive with a short half-life (roughly 12.3 years), so it is not naturally occurring in meaningful quantities on earth. A reactor will solve both of these problems with a *neutron blanket*, a neutron-absorbing structure surrounding the plasma. This provides the necessary shielding for sensitive reactor components. The heat generated in the blanket from neutron absorption will also be drawn off in a steam cycle to drive turbines, generating electricity from the reactor. Finally, seeding the blanket with lithium allows the following reactions with fusion neutrons:



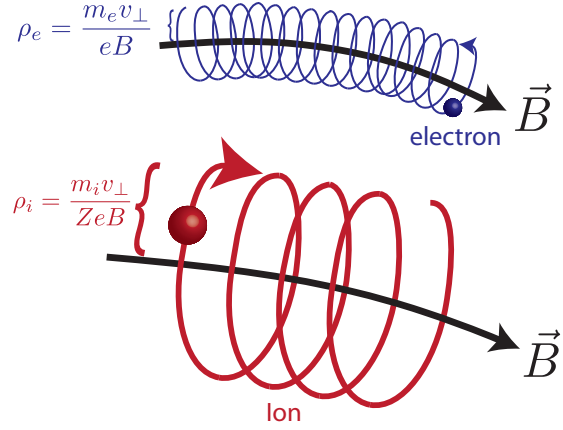
the Lithium-6 reaction (eq. (1.12)) absorbs “slow” neutrons (that is, neutrons that have thermalized to the blanket temperature via collisions) to produce tritium, plus additional heat. Lithium-7 (eq. (1.13)) is more likely to capture fast neutrons to produce tritium in an endothermic reaction; however, the reaction also acts as a neutron multiplier, as a free neutron is maintained through the reaction. Using blankets enriched with ${}^6\text{Li}$, coupled with neutron multipliers, a reactor will target an over-unity tritium breeding ratio, with > 1 tritons produced per neutron entering the blanket (i. e., per tritium consumed in a fusion reaction). •

1.2 MAGNETIC CONFINEMENT

1.2.1 Basic Principles

The temperatures in excess of 100 million Kelvin necessary for fusion in a plasma are inconsistent with any contact between solid reactor materials and the hot core of the plasma. Magnetic confinement relies on the strong response of the charged particles comprising the plasma to magnetic fields, rather than a material wall, to retain the thermal pressure (~ 10 atm for a reactor) from the plasma. The response of

Figure 1.3: Electron and ion gyro orbits in an applied magnetic field. Note that, due to the charge dependence in the Lorentz Force (eq. (1.14)), electrons and ions orbit in opposite directions relative to the magnetic field.



a charged particle to electric and magnetic fields is governed by the Lorentz force,

$$\vec{F} = q \left(\vec{E} + \vec{v} \times \vec{B} \right) \quad (1.14)$$

In a strong background magnetic field, the particle will move on a helical path along the magnetic field. The $\vec{v} \times \vec{B}$ factor in the Lorentz Force causes the particle to experience no magnetic force parallel to the field, while velocity perpendicular to the field generates a force proportional to the velocity times the magnetic field, directed perpendicular to both – thus the particle freely streams parallel to the field, but is trapped in a circular orbit perpendicular to it, termed “gyro motion”, as depicted in fig. 1.3. The particle will orbit at the cyclotron frequency,

$$\omega_c = \frac{qB}{m} \Rightarrow \omega_{ce} = \frac{eB}{m_e}, \quad \omega_{ci} = \frac{ZeB}{m_i} \quad (1.15)$$

for electrons and ions of charge Z , respectively (note that for brevity we indicate the magnitude of vectors as scalar variables, e.g., $B = |\vec{B}|$). A particle with velocity perpendicular to the magnetic field v_\perp (formally, $v_\perp = |\vec{v} \times \vec{B}|/B$) orbits at its gyroradius,

$$\rho = \frac{v_\perp}{\omega_c} = \frac{mv_\perp}{qB} \quad (1.16)$$

For a thermalized plasma, the perpendicular velocity will, on average, be the thermal velocity $v_t = \sqrt{2T/m}$, thus

$$\rho = \frac{\sqrt{2mT}}{qB} \quad (1.17)$$

The introduction of a nonzero electric field drives additional motion for the particle in the form of a drift velocity – the guiding center (that is, the average point about which the orbital motion of the particle gyrates) will shift with a bulk velocity (see [6, §8.4] for derivation)

$$\vec{v}_d = \frac{\vec{E} \times \vec{B}}{B^2} \quad (1.18)$$

independent of particle charge, mass, or energy.

This restriction of particle motion perpendicular to field lines to short length scales (at fusion-relevant temperatures and magnetic fields, the gyroradius is typically $\sim 10^{-5}$ m for electrons and $\sim 10^{-3}$ m for ions) compared to the size of the plasma is central to the premise of magnetic confinement. In the perpendicular direction, this scale restriction of particle motion permits a fluid treatment of the dynamics of the plasma. Further simplification of the fluid model (see [10, §2.3] for detailed derivation) leads to the theory of *magnetohydrodynamics* (MHD), the “workhorse” model describing plasma behavior. A basic equilibrium in a confined plasma is described in MHD by the simple relation

$$\nabla p = \vec{j} \times \vec{B} \quad (1.19)$$

in which the outward force due to the plasma pressure gradient is balanced by an inward force from the interplay between magnetic fields and electric currents (expressed by the current density \vec{j}). This interplay is readily illustrated in the simple one-dimensional case of an infinite straight cylinder of plasma – in this case, the radially-outward ∇p force may be balanced by an axial current in the \hat{z} direction with an azimuthal $\hat{\phi}$ magnetic field (z-pinch), an axial current and azimuthal field (θ -pinch), or a superposition of the two (screw pinch). However, all three of these options suffer from a lack of parallel confinement – as the magnetic field does not restrict the free-streaming parallel motion of the plasma, these linear concepts (when reduced to a physical, non-infinite size!) suffer from plasma losses at the ends of the cylinder. Despite efforts to restrict the parallel motion in a linear device (e.g., the “magnetic mirror,” which pinches the magnetic field at the cylinder ends in order to reflect the parallel motion of particles with a force due to the field gradient [11]), end losses in linear

devices proved incompatible with steady-state fusion conditions. The clear solution, then, was to close the magnetic geometry such that the magnetic field lines have no ends: a *torus*.

1.2.2 Toroidal Configurations

do this!!!

1.3 ALCATOR C-MOD

The data presented in this thesis were collected on the Alcator C-Mod tokamak [12, 13] at the MIT Plasma Science and Fusion Center. The Alcator series of tokamak experiments were designed as compact, high-field tokamaks. Despite its physical size (67 cm major radius, 22 cm minor radius, considerably smaller than other major experiments), Alcator C-Mod plasmas are capable of reaching ITER- and reactor-relevant densities ($> 1 \times 10^{20} \text{ m}^{-3}$) and pressures ($> 1 \text{ atm}$). This compact design is enabled by a very high toroidal magnetic field, reaching as high as 8.1 T, with typical operation near 5.5 T, driven by liquid-Nitrogen-cooled copper coils. C-Mod plasmas are primarily heated by ion-cyclotron (ICRF) heating **find cite!**, with up to 6 MW of heating power, with an additional $\sim 1 \text{ MW}$ of lower-hybrid resonance (LHRF) power used for heating and DC current drive [14]. A cutaway view of C-Mod, including support structures and the concrete “igloo” housing the cooling systems, is visible in fig. 1.4.

Table 1: Summary of Alcator C-Mod typical operating parameters.

<i>parameter</i>	<i>range</i>
major radius	0.67 m
minor radius	0.22 m
toroidal field	3 – 8.1 T
plasma current	$\leq 2 \text{ MA}$
plasma density	$\leq 5 \times 10^{20} \text{ m}^{-3}$
central temperature	$\leq 8 \text{ keV}$
plasma pressure	$\leq 2 \text{ atm}$
ICRF power	6 MW
LHRF power	1 MW

generate
cross-section figure
with labels

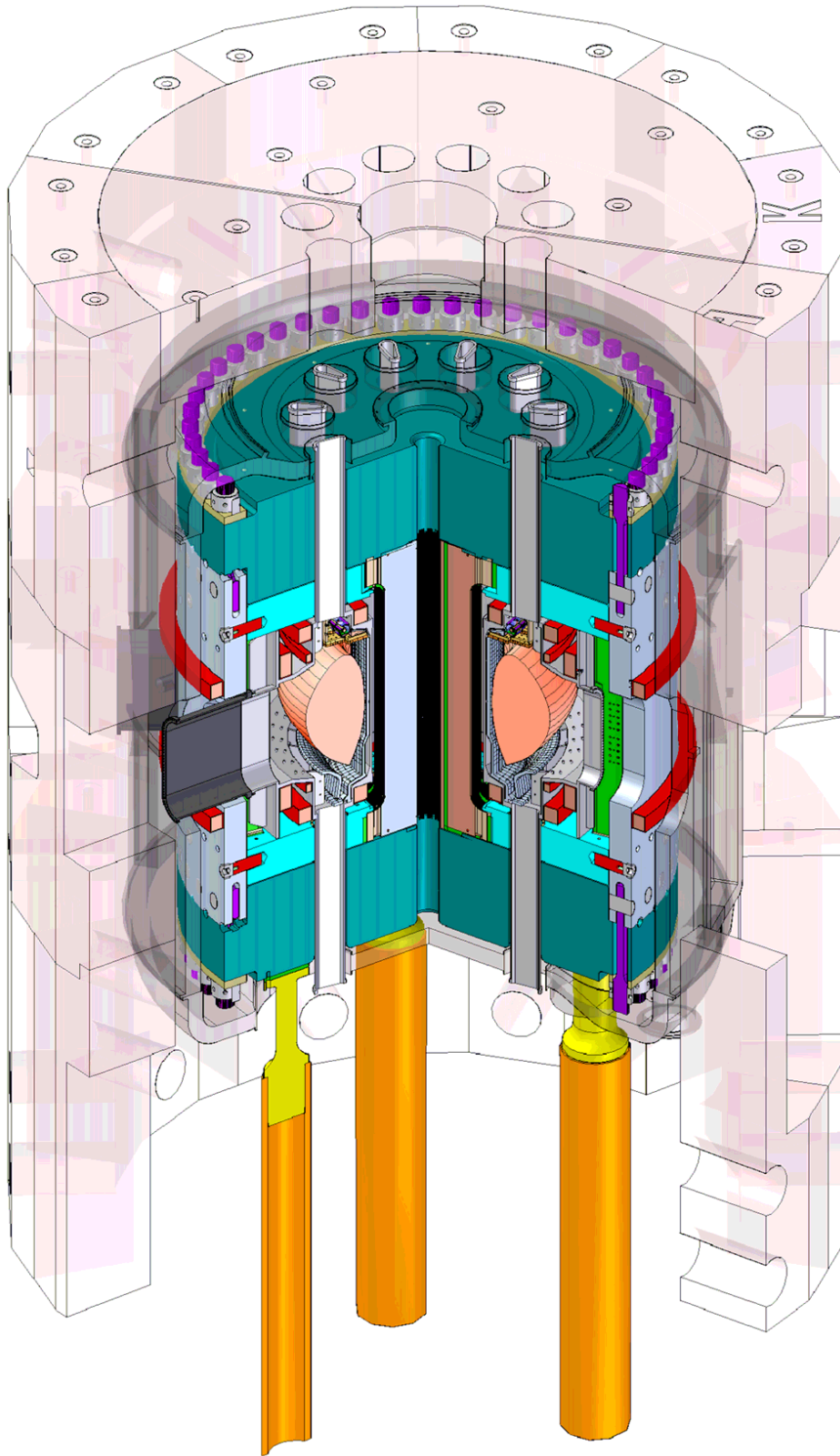


Figure 1.4: Cutaway view of the Alcator C-Mod tokamak, including cryostat and ancillary structures, illustrating the extensive support structures necessary for compact, high-field operation.

1.4 CONFINEMENT & TRANSPORT

1.4.1 *Global Confinement*

1.4.2 *Transport Barriers*

1.5 HIGH-PERFORMANCE REGIMES

1.5.1 *ELMy H-Mode*

1.5.2 *EDA H-Mode*

1.5.3 *I-Mode*

1.6 GOALS & OUTLINE

BIBLIOGRAPHY

- [1] United Nations. *World Population Prospects: The 2010 Revision. Comprehensive Tables*, volume 1. United Nations, 2010.
- [2] J. Klugman et al. *Human development report 2011. Sustainability and Equity: A Better Future for All*, 2011.
- [3] H. Gruenspecht. *International energy outlook 2011*. Center for Strategic and International Studies, 2010.
- [4] B.P. Global. *Statistical review of world energy 2010*.
- [5] U.S. Energy Information Administration. *Annual coal report 2012*, 2013.
- [6] J.P. Freidberg. *Plasma Physics and Fusion Energy*. Cambridge University Press, 2007.
- [7] J. Wesson. *Tokamaks*. International Series of Monographs on Physics. Oxford University Press, 2011.
- [8] F.F. Chen. *Introduction to Plasma Physics and Controlled Fusion*. Springer, 1984.
- [9] K.S. Krane. *Introductory Nuclear Physics*. Wiley, 1987.
- [10] J.P. Freidberg. *Ideal Magnetohydrodynamics*. Springer, 1987.
- [11] J. Kesner, R.S. Post, B.D. McVey, and D.K. Smith. *A tandem mirror with axisymmetric central-cell ion confinement*. *Nuclear Fusion*, 22(4):549, 1982.
- [12] I. H. Hutchinson, R. Boivin, F. Bombarda, P. Bonoli, S. Fairfax, C. Fiore, J. Goetz, S. Golovato, R. Granetz, M. Greenwald, S. Horne, A. Hubbard, J. Irby, B. LaBombard, B. Lipschultz, E. Marmor, G. McCracken, M. Porkolab, J. Rice, J. Snipes, Y. Takase, J. Terry, S. Wolfe, C. Christensen, D. Garnier, M. Graf, T. Hsu, T. Luke, M. May, A. Niemczewski, G. Tinios, J. Schachter, and J. Urbahn. *First results from alcator-c-mod*. *Physics of Plasmas*, 1(5):1511–1518, 1994.
- [13] M. Greenwald, N. Basse, P. Bonoli, R. Bravenec, E. Edlund, D. Ernst, C. Fiore, R. Granetz, A. Hubbard, J. Hughes, I. Hutchinson, J. Irby, B. LaBombard, L. Lin, Y. Lin, B. Lipschultz, E. Marmor, D. Mikkelsen, D. Mossessian, P. Phillips, M. Porkolab, J. Rice, W. Rowan, S. Scott, J. Snipes, J. Terry, S. Wolfe, S. Wukitch, and K. Zhurovich. *Confinement and transport research in alcator c-mod*. *Fusion Science and Technology*, 51(3):266–287, 2007.

- [14] J.R. Wilson, R. Parker, M. Bitter, P.T. Bonoli, C. Fiore, R.W. Harvey, K. Hill, A.E. Hubbard, J.W. Hughes, A. Ince-Cushman, C. Kessel, J.S. Ko, O. Meneghini, C.K. Phillips, M. Porkolab, J. Rice, A.E. Schmidt, S. Scott, S. Shiraiwa, E. Valeo, G. Wallace, J.C. Wright, and the Alcator C-Mod Team. **Lower hybrid heating and current drive on the alcator c-mod tokamak.** *Nuclear Fusion*, 49(11):115015, 2009.

COLOPHON

This document was typeset using `classicthesis` developed by André Miede (although aspects were changed to comply with the MIT thesis standards and the author’s personal preferences). The style was inspired by Robert Bringhurst’s seminal book on typography “*The Elements of Typographic Style*”. `classicthesis` is available for both \LaTeX and \LyX :

<http://code.google.com/p/classicthesis/>

Hermann Zapf’s *Palatino* and *Euler* type faces (Type 1 PostScript fonts *URW Palladio L* and *FPL*) are used. The “typewriter” text is typeset in *FPL*, originally developed by Bitstream, Inc. as “Bitstream Vera”. (Type 1 PostScript fonts were made available by Malte Rosenau and Ulrich Dirr.)